



A core-shell structured, metal–ceramic composite-supported Ru catalyst for methane steam reforming

Hyun Chul Lee^a, Yulia Potapova^a, Doohwan Lee^{b,*}

^aEnergy Lab, Emerging Technology Research Center, Samsung Advanced Institute of Technology, Samsung Electronics Co., LTD, Mt. 14-1, Nongseo-dong, Giheung-gu, Yongin, Gyeonggi-do 446-712, Republic of Korea

^bCatalysis and Nanomaterials Lab, Department of Chemical Engineering, University of Seoul, Siripdae-gil 13, Dongdaemun-gu, Seoul 130-743, Republic of Korea

H I G H L I G H T S

- Hydrothermal oxidation of Al metal particles was carried out at elevated temperatures.
- It formed a core-shell structured $\text{Al}_2\text{O}_3/\text{Al}$ metal–ceramic composite.
- The structure offered superior heat conductivity, surface area, and hierarchal pores.
- We used it as a support of ruthenium catalyst for methane steam reforming.
- The catalyst resulted in significantly enhanced hydrogen production yields.

A R T I C L E I N F O

Article history:

Received 7 March 2012

Received in revised form

29 April 2012

Accepted 21 May 2012

Available online 1 June 2012

Keywords:

Core-shell catalyst

Metal–ceramic composite

Fuel processing

Fuel cell

A B S T R A C T

Methane steam reforming on a metal–ceramic composite-supported ruthenium catalyst is studied at high temperatures. The core-shell structured $\text{Al}_2\text{O}_3/\text{Al}$ composite consisting primarily of an Al metal core with a high surface area $\gamma\text{-Al}_2\text{O}_3$ overlayer is obtained by hydrothermal oxidation. Under the synthesis condition, primary $\text{Al}_2\text{O}_3/\text{Al}$ particles aggregate to form a hierarchal secondary structure with macrosized inter-pores. This core-shell composite support enhances the heat conductivity and provides a high surface area for fine dispersion of a catalytic Ru component on the $\gamma\text{-Al}_2\text{O}_3$ overlayer. The Ru/ $\text{Al}_2\text{O}_3/\text{Al}$ catalyst exhibits significantly higher CH_4 conversion than the conventional Ru/ Al_2O_3 catalyst, indicating its superior properties for methane steam reforming at high temperatures contributed due to the fine Ru dispersion and facilitated heat and mass transfer via the unique catalyst structure. This metal–ceramic composite catalyst is stable in the reforming reaction for an extended time, suggesting reasonable stability in its physicochemical properties.

© 2012 Elsevier B.V. All rights reserved.

1. Introduction

Catalytic methane steam reforming (MSR, $\text{CH}_4 + \text{H}_2\text{O} \rightleftharpoons 3\text{H}_2 + \text{CO}$) is one of the most practiced and economically competitive methods for hydrogen production [1]. As a clean fuel, the demands for hydrogen are expected to rapidly grow with emerging fuel cells being used as an efficient power generation alternative [2,3]. We recently presented a compact and highly efficient fuel processor that provides H_2 fuel to residential fuel cell power systems by catalytic steam reforming of natural gas followed by water gas shift (WGS, $\text{CO} + \text{H}_2\text{O} \rightleftharpoons \text{H}_2 + \text{CO}_2$) and preferential CO oxidation (PROX, $\text{CO} + 1/2\text{O}_2 \rightarrow \text{CO}_2$) reactions [4]. These catalytic reactions are widely practiced in large petrochemical industries; however, several new technological challenges arise with

intensive integration of these processes into a small reactor assembly for fuel cell applications [5,6]. One implication is the intensification of the heat and mass transfer to deliver sufficient reaction enthalpies and reactant species to not limit the reaction conversion or selectivity under high space velocity conditions. This intensification is markedly important to achieve enhanced H_2 throughput in a compact reactor system of fuel cells. For example, MSR is highly endothermic ($\Delta H_{298} = 206 \text{ kJ mol}^{-1}$), whereas CO oxidation is extremely exothermic ($\Delta H_{298} = -283 \text{ kJ mol}^{-1}$) [7]. Therefore, improper heat management in a fuel processor results in inefficiently low CH_4 conversion and scariification of the CO oxidation selectivity by the hydrogen oxidation side reaction. This would in turn lead to a decrease in the overall efficiency and operation dynamics of the fuel cell system. Application of a micro-channel reactor design is an effective approach to increase the surface area to volume ratio in catalytic fuel processors. However, heat transport through the packed catalyst bed in the inner channels of the reactor may play as a performance determining factor considering that

* Corresponding author. Tel.: +82 2 2210 5369; fax: +82 2 2210 5271.
E-mail address: dolee@uos.ac.kr (D. Lee).

industrial heterogeneous catalysts generally consist of solid oxides of low heat conductivity as support material.

In this study, we present properties of a highly heat conductive, core-shell structured, metal–ceramic composite catalyst for MSR at high temperatures. The catalyst support consisted of an Al metal core encapsulated by a hydrothermally-grown, high surface area γ - Al_2O_3 shell, designated as $\text{Al}_2\text{O}_3@\text{Al}$. The hydrothermal synthesis of Al– Al_2O_3 metalloceramics was pioneered by Tikhov [8–10]. However, only a few studies have investigated their applications as catalysts [11,12]. The aim of this work is to investigate the properties of the metal–ceramic $\text{Al}_2\text{O}_3@\text{Al}$ composite as a catalyst support in MSR, which requires enhanced heat conductivity and surface properties of the catalyst to achieve enhanced fuel processing in fuel cells. A ruthenium catalyst supported on the $\text{Al}_2\text{O}_3@\text{Al}$ was prepared for the highly endothermic MSR, and the results were compared to a conventional Al_2O_3 supported Ru catalyst.

2. Experimental

An $\text{Al}_2\text{O}_3@\text{Al}$ core-shell structured support was prepared by hydrothermal surface oxidation of aluminum metal powder (Goodfellow, mean particle size $\leq 25 \mu\text{m}$). The Al powder was placed into a specially designed, stainless steel compartment that provided excess water vapor and contraction forces among the particles during the hydrothermal treatment. The hydrothermal oxidation was conducted in an autoclave at 473 K for 6 h under an autogenous pressure of approximately 2.7 MPa. The product was then dried at 373 K in air, and the final form of the core-shell structured $\text{Al}_2\text{O}_3@\text{Al}$ composite was obtained after dehydration by calcination in air at 823 K for 4 h. A ruthenium catalyst (2 wt% Ru) was prepared using this $\text{Al}_2\text{O}_3@\text{Al}$ sample as a support by a conventional wet impregnation method. Excess aqueous RuCl_3 solution ($\sim 19.8 \text{ mM Ru}$) was prepared dissolving 1.0 g of ruthenium chloride hydrate (Aldrich) in 100 ml of deionized water, and mixed with 20 g of the $\text{Al}_2\text{O}_3@\text{Al}$ at RT under vigorous stirring for 6 h. The sample was then dried in a rotary vacuum evaporator at 337 K and subsequently in a convection oven at 373 K for 12 h under atmospheric condition. No additional step was applied for elimination of chlorine from the catalysts. The final form of the Ru/ $\text{Al}_2\text{O}_3@\text{Al}$ catalyst was obtained after calcination in air at 973 K for

4 h (ramp = 10 K min^{-1}), and subsequent reduction in H_2 at 973 K for 1 h.

The structural characteristics of the $\text{Al}_2\text{O}_3@\text{Al}$ support and Ru/ $\text{Al}_2\text{O}_3@\text{Al}$ catalyst were investigated with powder X-ray diffraction (XRD), scanning electron microscopy (SEM), field emission transmission electron microscopy (FE-TEM), and N_2 adsorption-desorption methods. Crystallographic XRD patterns of the samples were obtained with Cu K α radiation operated at 40 kV and 40 mA (Philips X'pert X-ray diffractometer). The morphologies of the samples were obtained by SEM (Hitachi-S2400) and FE-TEM (Tecnai-F20) operated at 200 kV. The surface area and pore size of the samples were calculated, respectively, with Brunauer-Emmett-Teller (BET) and Barrett-Joyner-Halenda (BJH) methods using N_2 adsorption-desorption isotherms obtained in a volumetric unit (Tristar 3000, Micromeritics). The methane steam reforming was conducted on the Ru/ $\text{Al}_2\text{O}_3@\text{Al}$ catalyst at atmospheric pressure in a fixed bed quartz glass reactor of tubular geometry with an outside diameter (OD) of 20 mm, wall thickness of 1 mm (ID = 18 mm), and length of 500 mm. Fig. 1 shows schematic of the reactor and equipment set up for methane steam reforming. The catalysts were pelletized to diameters between 1.7 and 2.4 mm, considering that fuel processing catalysts are fabricated to large sizes to minimize pressure-drop through the catalyst bed in practical reactor applications. The catalysts were packed in the middle of the reactor fixing the position using quartz wool. The reactor was installed in a PID controlled tubular electric furnace (450 mm length), and the temperature of the reactor was measured and controlled attaching a thermocouple onto the outside wall of the reactor at the catalyst bed section. The catalysts were reduced in H_2 at 973 K for 1 h before the reforming reaction. The CH_4 and H_2O vapor stream was premixed passing through a pre-heater at constant temperature of 673 K, and introduced to the reactor at a $\text{H}_2\text{O}/\text{CH}_4$ (S/C) mole ratio of 3.0 which is 1.5 times higher than the theoretically required stoichiometry ratio for the reaction ($\text{S}/\text{C} = 2.0$, $\text{CH}_4 + 2\text{H}_2\text{O} \rightleftharpoons \text{CO}_2 + 4\text{H}_2$). The feed rate of this reactant mixture was varied to 0.98, 1.96, and 3.93 mol h^{-1} using an HPLC pump (LabAlliance, Series II) and a mass flow controller (Brooks 5850E) unit. The reforming reaction was conducted at 873 and 973 K under three different gas hourly space velocity (GHSV) conditions of 8000, 16,000, and $32,000 \text{ h}^{-1}$. The effluents were analyzed online using a multi-component real-time, non-

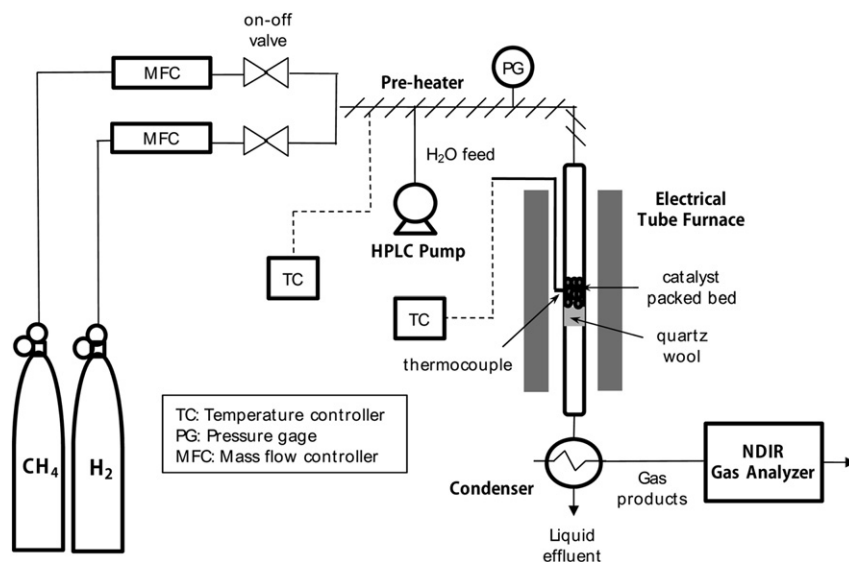


Fig. 1. Schematic of the reactor and equipment set up for catalytic methane steam reforming (MSR).

dispersive infrared (NDIR) gas analyzer unit (NGA 2000, MLT-4, Rosemount analyzer system). For comparison, the reaction was also conducted over a commercial Ru catalyst supported on Al_2O_3 (2 wt% Ru, Süd-Chemie) at the same loading amount of the catalyst and the reaction condition applied for Ru/ Al_2O_3 @Al catalyst. A blank MSR experiment conducted at 873 and 973 K with inert quartz chips loaded in the reactor did not show methane conversion indicating that homogeneous MSR or methane decomposition reactions were not likely to occur or negligible at these conditions. The ruthenium contents in the Ru/ Al_2O_3 @Al and the commercial Ru/ Al_2O_3 catalysts were measured by inductively coupled plasma – atomic emission spectroscopy (ICP-AES, JY-70Plus, Jobin-Yvon). Dispersions of Ru on the catalysts were obtained by CO chemisorption at 308 K after pre-reduction of the samples in H_2 at 973 K for 1 h (Autochem 2910, Micromeritics).

3. Results and discussion

The core-shell structured Al_2O_3 @Al composite consisting primarily of an Al metal core encapsulated by a thick $\gamma\text{-Al}_2\text{O}_3$ overlayer was developed by hydrothermal surface oxidation of Al metal particles. Fig. 2 shows the structure and morphology of the Al_2O_3 @Al samples obtained by (a) SEM and (b) FE-TEM, respectively. The results revealed that the Al_2O_3 overlayer consisted of aggregated small crystallites of rod-like geometries, which preferentially developed perpendicular to the Al metal surface. The aggregation of these oxide crystallites appeared to be very dense, forming a thick Al_2O_3 overlayer with a thickness in the range of 0.6 and 1.5 μm .

Fig. 3 displays the powder XRD patterns on the Ru/ Al_2O_3 @Al catalysts. To investigate the phase composition and stability, the XRD patterns were obtained for (a) fresh and (b) used catalysts for

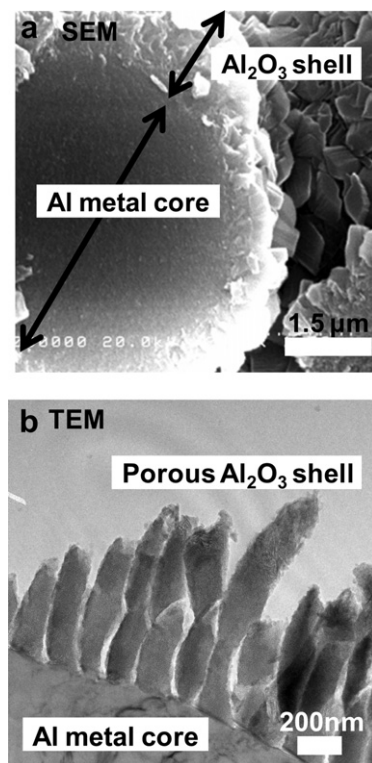


Fig. 2. Structure and surface morphology of the core-shell structured Al_2O_3 @Al composite obtained by (a) Scanning Electron Microscopy (SEM) and (b) Field Emission Transmission Electron Microscopy (FE-TEM).

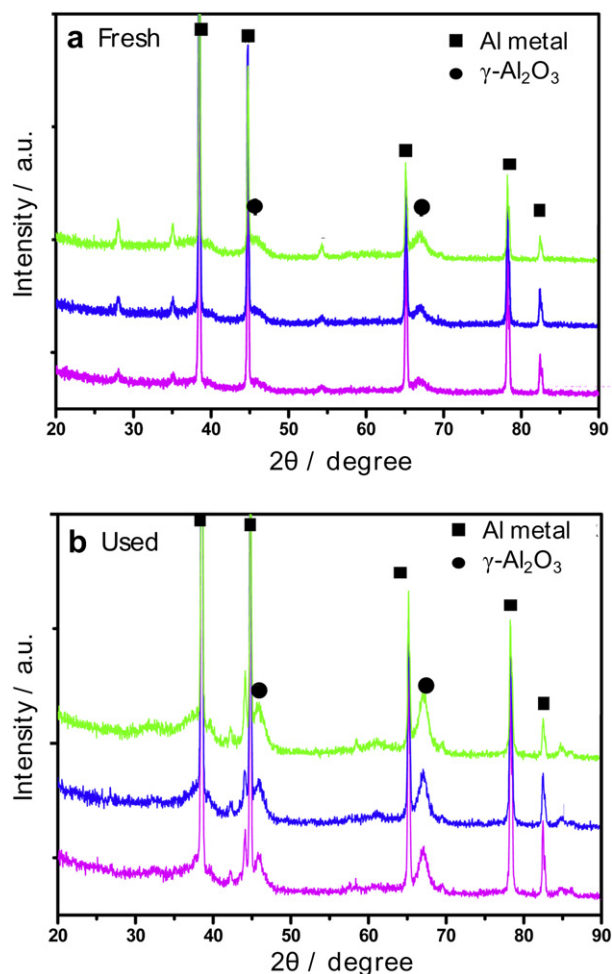


Fig. 3. Powder X-ray diffraction patterns on three different batches of the Ru/ Al_2O_3 @Al catalysts (2 wt% Ru); (a) fresh catalysts (b) catalysts used in the reforming reaction at 973 K over 60 h ($S/C = 3.0$, $\text{GHSV} = 8000 \text{ h}^{-1}$). For a consistent analysis, three different batches of the samples were obtained and applied for MSR reaction at the same conditions.

the reforming reaction (973 K , $S/C = 3$, $\text{GHSV} = 8000 \text{ h}^{-1}$) over 60 h. For consistent analysis, three different batches of the samples were obtained and used for the reaction at the same condition. The XRD results clearly indicated the co-presence of the Al metal and the $\gamma\text{-Al}_2\text{O}_3$ in both the fresh and used catalysts, reflecting the construction and sustainability of the $\gamma\text{-Al}_2\text{O}_3$ @Al composites. Diffraction peaks corresponding to the Ru metal or oxides were not observed, suggesting fine dispersion of the Ru species as small nanoparticles over the surface of the $\gamma\text{-Al}_2\text{O}_3$ overlayer. The Ru fractional dispersion on the catalyst obtained by CO chemisorption was approximately 0.14, confirming fine dispersion of Ru on the Al_2O_3 @Al support. The phase composition of Al and $\gamma\text{-Al}_2\text{O}_3$ in the Ru/ Al_2O_3 @Al was estimated by a correlation of the area ratio of Al and $\gamma\text{-Al}_2\text{O}_3$ diffraction peaks to the predetermined calibration values measured with mixtures of Al and $\gamma\text{-Al}_2\text{O}_3$ powders at various ratios. This analysis produced approximately 34 wt% $\gamma\text{-Al}_2\text{O}_3$ phase in the fresh Ru/ Al_2O_3 @Al sample. Assuming a spherical core-shell geometry of the Al_2O_3 @Al support, the average thickness of the $\gamma\text{-Al}_2\text{O}_3$ overlayer was estimated using the phase contents and theoretical density of Al (2.70 g cm^{-3}) and $\gamma\text{-Al}_2\text{O}_3$ (3.60 g cm^{-3}) [13]. This simple calculation led to the average $\gamma\text{-Al}_2\text{O}_3$ overlayer thickness of approximately 0.5–1.1 μm for a Al_2O_3 @Al diameter of 10–20 μm . Noticeably, this estimated γ -

Al_2O_3 overlayer thickness was within the values directly observed by SEM and TEM, which showed good agreement. The $\gamma\text{-Al}_2\text{O}_3$ phase content in the $\text{Ru}/\text{Al}_2\text{O}_3/\text{Al}$ catalyst used for CH_4 reforming (973 K, $\text{S}/\text{C} = 3$, $\text{GHSV} = 8000 \text{ h}^{-1}$, 60 h) was approximately 38 wt%, increasing by approximately 4 wt% from the initial value in the fresh catalyst. This change in the content of the $\gamma\text{-Al}_2\text{O}_3$ phase was reasonable considering the catalyst was exposed to MSR at high temperature for an extended time, in which the oxidation and reduction species co-existed in the reformat stream. However, the change in $\gamma\text{-Al}_2\text{O}_3$ content on the used catalyst was much less than that expected under a hydrothermal environment. A few reasonable explanations are suggested. First, the diffusion of oxidant species through the Al_2O_3 overlayer to the surface of the Al metal core would be difficult as the dense oxide overlayer formed and grew gradually into a thick layer. Second, a portion of the oxidant species adsorbed to the catalyst surface would continuously convert into the product species by the reforming reaction. In addition, the reforming product stream contained large amounts of hydrogen and carbon monoxide, which may hinder the oxidation of Al to Al_2O_3 .

Fig. 4 compares SEM images of (a) fresh and (b) used $\text{Ru}/\text{Al}_2\text{O}_3/\text{Al}$ catalysts for the MSR reaction (973 K, $\text{S}/\text{C} = 3.0$, $\text{GHSV} = 8000 \text{ h}^{-1}$) over 60 h. The images on the fresh catalyst displayed a hierarchal secondary structure consisting of $\text{Al}_2\text{O}_3/\text{Al}$ particles strongly aggregated by the inter-grown γ -alumina on the surface of the Al metal particles by hydrothermal oxidation under a compression environment. The macroscale inter-pores between the primary $\text{Al}_2\text{O}_3/\text{Al}$ particles were clearly developed. This overall morphology remained after extended exposure to the high temperature methane steam reforming. The SEM image on the used catalyst in Fig. 4(b) displayed a composite structure similar to that on the fresh catalyst. The inset image taken by Energy Dispersive

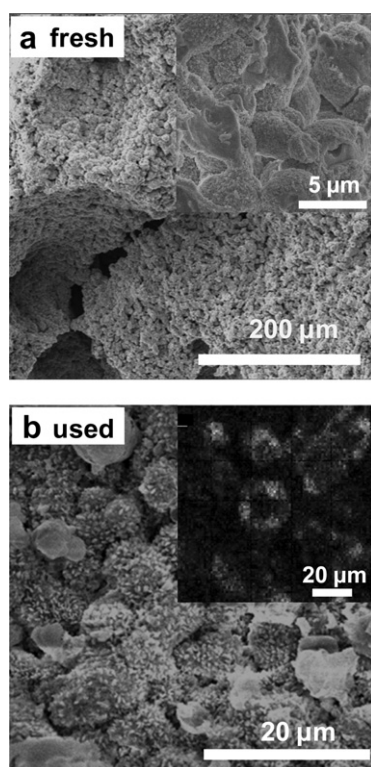


Fig. 4. a) SEM image on the fresh $\text{Ru}/\text{Al}_2\text{O}_3/\text{Al}$ catalyst, inset: SEM images at higher resolution. b) SEM image on the used $\text{Ru}/\text{Al}_2\text{O}_3/\text{Al}$ catalyst (973 K, $\text{S}/\text{C} = 3.0$) in the methane steam reforming over 60 h, inset: EDX composition analysis results (The bright area indicates the oxide phase encapsulating the Al metal core).

X-ray (EDX) analysis confirmed the presence of Al metal grains encapsulated by Al_2O_3 phases, preserving the core-shell structure.

The XRD, SEM, TEM, and EDX results collectively indicate reasonable physicochemical stability of the $\text{Al}_2\text{O}_3/\text{Al}$ composite as a catalyst support for high temperature MSR. The net BET surface area on the $\gamma\text{-Al}_2\text{O}_3$ overlayer was estimated by the measured surface area of the $\text{Al}_2\text{O}_3/\text{Al}$ composite and the $\gamma\text{-Al}_2\text{O}_3$ phase content obtained from XRD analysis. This analysis revealed that the surface area of the oxide overlayer was approximately $200 \text{ m}^2 \text{ g}^{-1}$, and the pore volume of the composite was approximately $0.4 \text{ m}^3 \text{ g}^{-1}$. The SEM, TEM, and XRD results in this study suggest that the alumina overlayer developed as crystallized aggregates that appeared to be pseudomorphous to boehmite, formed by the hydrothermal oxidation. Similar microstructures in the hydrothermally-obtained $\text{Al}-\text{Al}_2\text{O}_3$ composites were previously reported in which the oxide crystallites consisted of platelets stacked along the $\langle 110 \rangle$ direction and separated by slit-shaped pores that produced high surface area micropores [9]. The $\text{Al}_2\text{O}_3/\text{Al}$ composite obtained in this work presents a unique core-shell primary structure and a hierarchal secondary structure with a polymodal pore size distribution from macropores to micropores. Therefore, the superior heat conductivity and surface properties of the $\text{Al}_2\text{O}_3/\text{Al}$ composite constructively contribute to the catalytic property of the $\text{Ru}/\text{Al}_2\text{O}_3/\text{Al}$ catalyst.

The catalytic properties of the $\text{Ru}/\text{Al}_2\text{O}_3/\text{Al}$ catalyst (2 wt% Ru) for MSR were compared to those of a commercial $\text{Ru}/\text{Al}_2\text{O}_3$ hydrocarbon reforming catalyst (2 wt% Ru, Süd-Chemie). The ruthenium contents in these catalysts were confirmed by ICP-AES analysis, in which the measured Ru contents were close to 2 wt% (± 0.04) agreeing well with the expected value. The Ru dispersions on these catalysts measured by CO chemisorption were similar with approximate values of 0.14. Fig. 5 displays CH_4 conversions and hydrogen production yields on these catalysts under the MSR reaction at (a) 873 and (b) 973 K for various GHSV conditions of 8000, 16,000, and $32,000 \text{ h}^{-1}$ ($\text{S}/\text{C} = 3.0$). The theoretical CH_4 equilibrium conversions at these reaction conditions are also shown. The catalyst loading amount and pellet sizes were the same, and the Ru dispersions on these catalysts were also similar. The $\text{Ru}/\text{Al}_2\text{O}_3/\text{Al}$ catalyst showed considerably greater CH_4 conversion than the $\text{Ru}/\text{Al}_2\text{O}_3$ catalyst at the temperature and GHSV conditions applied in this work. The enhancement in CH_4 conversion on the $\text{Ru}/\text{Al}_2\text{O}_3/\text{Al}$ catalyst was greater at elevated GHSV conditions. The decrease in CH_4 conversion with an increase in the space velocity on all of the catalysts was reasonable considering that the total reactant feed with a given amount of catalyst increased at elevated GHSV conditions. However, the results indicated that hydrogen production yields actually increased at higher space velocity conditions. The enhancement in CH_4 conversion on the $\text{Ru}/\text{Al}_2\text{O}_3/\text{Al}$ compared to the $\text{Ru}/\text{Al}_2\text{O}_3$ catalyst suggested that an enhanced heat transfer through the highly heat conductive $\text{Ru}/\text{Al}_2\text{O}_3/\text{Al}$ catalyst packed in the reactor constructively contributed to the reaction by facilitated delivery of the reaction enthalpy for the reaction to proceed. Such effects decreased as the conversion approached equilibrium, as expected from the reaction kinetics. The net reaction rate decreased gradually as the reaction approaches to the thermodynamic equilibrium; therefore the required net reaction enthalpy decreased. The thermal conductivity of dense aluminum metal is $247 \text{ W m}^{-1} \text{ K}^{-1}$ while that of dense aluminum oxide is $39 \text{ W m}^{-1} \text{ K}^{-1}$ at 373 K [14]. It is reasonably expected from these theoretical values that the metal–ceramic-composite $\text{Ru}/\text{Al}_2\text{O}_3/\text{Al}$ catalyst would provide much higher heat conductivity than the $\text{Ru}/\text{Al}_2\text{O}_3$ catalyst. However, a precise evaluation of heat conductivity through the catalyst pellets packed in the reactor is difficult, because it also depends on particle sizes and packing density etc. In addition, it should be noticed that MSR reaction was conducted under non-equilibrium states throughout the experiments in this study. Therefore, it is the heat flux

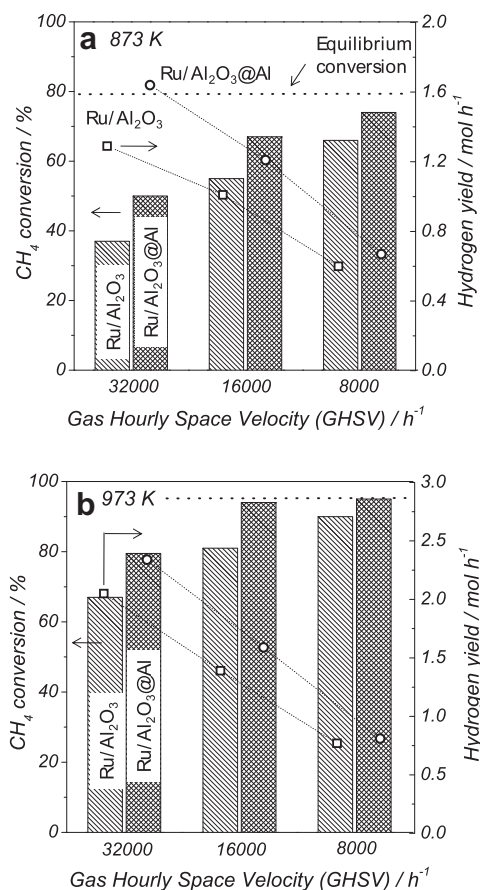


Fig. 5. CH₄ conversion and hydrogen yield on the Ru/Al₂O₃@Al and Ru/Al₂O₃ catalysts in methane steam reforming reaction (S/C = 3.0) at various GHSV conditions. The theoretical equilibrium conversion is presented as a dot line. Reaction temperature; a) 873 K, and b) 973 K.

through the catalyst packed-bed, not the temperature gradient, which should be correlated to the level of methane conversion for appropriate analysis. It leads to a conclusion that measurement of temperature gradient across the catalyst bed does not provide decisive information, whereas the increment of methane conversion is the direct and appropriate indicative for the constructive contribution of enhanced heat conductivity of the metal–ceramic composite catalyst to the highly endothermic MSR reaction.

Fig. 6 displays the CH₄ conversion on the Ru/Al₂O₃@Al and Ru/Al₂O₃ catalysts in MSR measured for an extended time at 873 and 973 K. The results clearly show that the level of CH₄ conversion remained close to the initial value, indicating little deactivation of the catalysts by thermal sintering or carbon deposition under these reaction conditions. The steadily sustained CH₄ conversion level and the small change in the Al₂O₃ phase content observed on the Ru/Al₂O₃@Al catalyst after the reforming reaction suggested that the core-shell structure of the metal–ceramic composite was stable.

A common approach to obtain a metal–ceramic composite for a catalyst support is wash-coating of porous oxide layers on a metallic monolith; however, the product is usually prone to degradation at the metal–oxide interface. The analyses herein collectively suggest that the structure of the Al₂O₃@Al core-shell composite was stable. This composite can be synthesized relatively easily compared to the wash-coated monolith and is more convenient to fill as particles form in the narrow channels of a fuel processor where the surface to volume ratio of the reaction zone is intensified. This work suggests that the core-shell structured

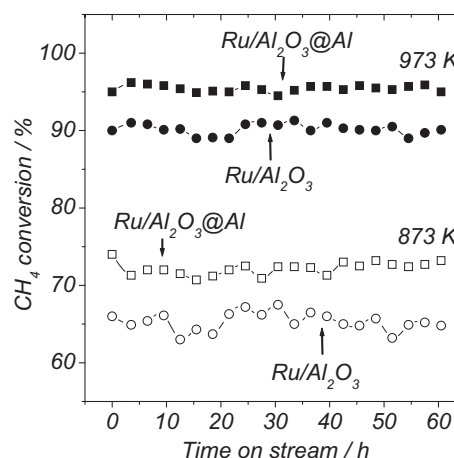


Fig. 6. CH₄ conversion on the Ru/Al₂O₃@Al and Ru/Al₂O₃ catalysts in methane steam reforming reaction for an extended time. The reaction was carried out at 873 K and 973 K, respectively (S/C = 3, GHSV = 8000 h⁻¹).

Al₂O₃@Al composite could be used as an efficient catalyst support for a variety of reactions where heat and mass transfer have significant roles.

4. Conclusions

The core-shell structured Al₂O₃@Al composite consisting of a highly heat conductive Al metal core and high surface area γ -Al₂O₃ overlayer with superior pore networks provided facile heat transfer with enhanced dispersion of an active Ru component. These properties enhanced the CH₄ conversion in MSR on the Ru/Al₂O₃@Al more than did the conventional Ru/Al₂O₃ catalyst. The properties of the Ru/Al₂O₃@Al showed little change during extended exposure to the reforming reaction, indicating reasonable stability of the structure. This metal–ceramic composite offers new opportunities as a catalyst support in a variety of areas, including fuel processing for fuel cells.

Acknowledgment

D. Lee gratefully acknowledges financial support from the University of Seoul in the form of a 2010 Research Fund (Grant 2010-04301005).

References

- [1] R.G. Lemus, J.M.M. Duart, *Int. J. Hydrogen Energy* 35 (2010) 3929–3936.
- [2] C.-J. Winter, *Int. J. Hydrogen Energy* 34 (2009) S1–S52.
- [3] M. Ball, M. Wietschel, *Int. J. Hydrogen Energy* 34 (2009) 615–627.
- [4] D. Lee, H.C. Lee, K.H. Lee, S. Kim, *J. Power Sources* 165 (2007) 337–341.
- [5] A. Qi, B. Peppley, K. Karan, *Fuel Process. Technol.* 88 (2007) 3–22.
- [6] J. Xuan, M.K.H. Leung, D.Y.C. Leung, M. Ni, *Renew. Sust. Energ. Rev.* 13 (2009) 1301–1313.
- [7] Y.H. Kim, E.D. Park, H.C. Lee, D. Lee, K.H. Lee, *Catal. Today* 146 (2009) 253–259.
- [8] S.F. Tikhov, A.N. Salanov, Y.V. Paleskaya, V.A. Sadykov, G.N. Kustova, G.S. Litvak, N.A. Rudina, V.A. Zaikovskii, S.V. Tsybulya, *React. Kinet. Catal. Lett.* 64 (1998) 301–308.
- [9] S.F. Tikhov, V.B. Fenelonov, V.I. Zaikovskii, Y.V. Potapova, V.A. Sadykov, *Microporous Mesoporous Mater.* 33 (1999) 137–142.
- [10] S.F. Tikhov, V.E. Romanenkov, V.A. Sadykov, V.N. Parmon, A.I. Rat'ko, *Kinet. Catal.* 46 (2005) 641–659.
- [11] N. Burgos, M. Paulis, M.M. Antxustegi, M. Nontes, *Appl. Catal. B: Environ.* 38 (2002) 251–258.
- [12] G. Patermarakis, N. Nicolopoulos, *J. Catal.* 187 (1999) 311–320.
- [13] J.E. McMurry, R.C. Fay, *Chemistry*, fifth ed. Pearson Prentice Hall, New Jersey, 2008.
- [14] W.D. Callister, D.G. Rethwisch, *Fundamentals of Materials Science and Engineering*, third ed., Wiley, New Jersey, 2008.